Scaling of energy deposition in central heavy-ion reactions at intermediate energies

Z. Basrak[1]*, *Ph. Eudes*[2], *M. Zorić*[1] *and F. Sébille*[2]
[1] Ruđer Bošković Institute, P.O.Box 180, HR-10 002 Zagreb, Croatia
[2] SUBATECH, EMN-IN2P3/CNRS-Université de Nantes, P.O.Box 20722, F-44 307 Nantes, France

Abstract
Semiclassical transport simulation of heavy-ion reactions (HIR) between about the Fermi energy and 100A MeV reveals a perfect linear correlation between the maximal excitation energy put into a nuclear system and the incident energy. This scaling feature becomes a universal property of HIR independent of reaction entrance channel parameters (system size, asymmetry and energy) when these excitation maxima are expressed in units of the system available energy. The constancy of the excitation energy fraction in the system available energy is on the best corroborate by those analysis of experimental data which do not presume a reaction mechanism dominating the collision process.

1 Introduction

For central HIR at low energies system undergoes fusion and fusion-like slow, essentially mean-field–transformation processes. With increasing incident energy $E_{\rm in}$ a much faster and considerably more violent reaction mechanism sets in and reaction becomes dominated by elementary nucleon-nucleon (NN) collisions. In fusion the entire available energy of the reaction is deposited via thermal excitation, whereas at higher energy a considerable fraction of the available energy is deposited into system via compression. By increasing $E_{\rm in}$ one expects that only a fraction of the available energy is effectively deposited into the reaction system and becomes dissipated during the reaction course. It is commonly admitted that this fraction should monotonically decrease with the increase of $E_{\rm in}$.

For $E_{\rm in}$ from about the Fermi energy $E_{\rm F}$ to several 100A MeV, the energy transformation is determined by those processes which govern heating and compression of a reacting system. The time scales involved are of the order of time which reaction partners need to bypass each other [1,2]. Projectile energy per nucleon $E_{\rm in}$ and reaction geometry (impact parameter and system mass asymmetry) determine the dominant reaction mechanism. Consequently, the course of a HIR is "decided" in the very first instances of a collision [3,4]. In central, the most violent collisions the largest fraction of the entrance channel energy is converted into internal degrees of freedom. Thus, the central collisions are of our greatest interest.

Table 1: Systems and energies studied for central collisions.

System	Incident energy (A MeV)
^{40}Ar+^{27}Al	25, 41, 53, 65, 77, 99
^{36}Ar+^{58}Ni	52, 74, 95
^{40}Ar+^{107}Ag	20, 30, 40, 45, 50, 75, 100
^{40}Ar+^{197}Au	50, 75, 100
^{36}Ar+^{36}Ar	32, 40, 52, 74
^{58}Ni+^{58}Ni	52, 74, 90
^{129}Xe+^{120}Sn	25, 32, 39, 45, 50, 75, 100
^{197}Au+^{197}Au	20, 30, 40, 60, 80, 100

We have shown theoretically that an intermediate energy HIR follows a two-stage scenario, a prompt first compact-stage and a second after-breakup one [4]. The emission pattern of central collisions is characterized by a copious and prompt dynamical emission occurring during the compact and prior-to-scission reaction phase [4–6]. This is the main system-cooling component and the amount of deposited energy into the compact system linearly increases with the projectile energy [7]. These results witness the above conclusion that global characteristics of HIR exit channel are determined in the first prompt reaction stage underlying the interest in studying the first instances of nuclear collisions.

*basrak@irb.hr

In this work we theoretically examine how much of the system energy may be temporarily stocked into the reaction system in the form of excitation energy as a function of $E_{\rm in}$, system size $A_{\rm sys}$ and system mass asymmetry. Four mass symmetric and four mass asymmetric central reactions were studied at several energies (see Tab. 1 for a review). Comparison with the pertinent results deduced from HIR experiments is presented too.

2 Transport model

Simulation was carried out within a semiclassical microscopic transport approach of Boltzmann's type using the Landau-Vlasov (LV) model [8]. The highly nonlinear LV equation $\frac{\partial f}{\partial t} + \{f, H\} = I_{\rm coll}(f)$ is solved by the test-particle method. $f(\mathbf{r}, \mathbf{p}; t)$ is the one-body density distribution function describing the spatio-temporal evolution of the system governed by the effective Hamiltonian H consisting of the self-consistent nuclear and Coulomb fields. The D1-G1 momentum-dependent interaction due to Gogny (the incompressibility module K_∞=228 MeV and the effective mass m^*/m=0.67) [9] was used to describe the nuclear mean-field potential. $\{\ ,\ \}$ stands for the Poisson brackets and $I_{\rm coll}$ is the collision integral. The effects of the Pauli-suppressed two-body residual NN collisions are treated on average in the Uehling-Uhlenbeck approximation taking the isospin- and energy-dependent free-scattering value for the NN cross section. Such an approach is very successful in reproducing a variety of global experimental dynamical observables because they are adequately described by the time evolution of the one-body density. Thus, the LV model is especially appropriate for describing the early stages of HIR, when the system is hot and compressed.

The observable studied is the thermal component (heat), i.e. one of the two main intrinsic-energy deposition components of the early-reaction-stage energy transformation. Heat is stocked into the compact system predominantly by NN collisions which occurs in the overlap zone. In the most of cases under study the time is too short for the full relaxation of the pressure tensor and establishment of a global equilibrium in momentum space. Therefore, it is more correct to name this component the excitation energy $E_{\rm x}$. Detailed definition of the transformation of the (system) available energy $E^{\rm c.m.}_{\rm avail}$ into intrinsic and collective degrees of freedom may be found elsewhere [7,10,11]. $E^{\rm c.m.}_{\rm avail}$ is defined as the center-of-mass system energy per nucleon $E^{\rm c.m.}_{\rm avail} = \frac{E_{\rm P}}{A_{\rm P}} \frac{A_{\rm P} A_{\rm T}}{(A_{\rm P}+A_{\rm T})^2}$, where $E_{\rm P}/A_{\rm P} = E_{\rm in}$ and $A_{\rm P}(A_{\rm T})$ is the projectile (target) number of nucleons.

3 Excitation energy versus incident energy

As an example of the time evolution of excitation energy per nucleon the inset of Fig. 1 shows $E_{\rm x}/A$ for the Au+Au reaction at six energies studied. Within a laps of time of merely 40–75 fm/c after the contact of colliding nuclei occurring at 0 fm/c the excitation energy per nucleon $E_{\rm x}/A$ reaches a maximum and then its value decreases almost as rapidly as it increased. The maxima are reached earlier and their height increases and width decreases with increasing $E_{\rm in}$. The regular and nearly symmetric rise and decrease of $E_{\rm x}/A$ with the reaction time is a common behavior for all reactions studied. The observed regularity suggests that maxima of $E_{\rm x}/A$ are proportional to the total energy deposited during HIR.

We are examining the maximal energy that may be dissipated in HIR. Thus, we take the maxima of $E_{\rm x}/A$ which we denote by $(E_{\rm x}/A)_{\rm max}$. The value of $(E_{\rm x}/A)_{\rm max}$ can readily and accurately be extracted from the simulation results. Figure 1 depicts how these maxima depends on $E^{\rm c.m.}_{\rm avail}$ for all studied HIR. Abscissa value is shifted for the threshold, the Coulomb barrier energy. With this correction the linear fit over all data points crosses abscissa axis closer to the origin of the graph. All data points lie very close to the fit line. One is facing a peculiar universal linear rise which is independent of $A_{\rm sys}$ and mass asymmetry in the full and a rather large span of $E_{\rm in}$ covered in this study.

An important question is whether the existing central HIR experimental data support our simulation results and in particular whether $E_{\rm x}$ linearly depends on $E_{\rm in}$. Most of the energy put into the system during the early reaction phase is released by the emission of particles and light and interme-

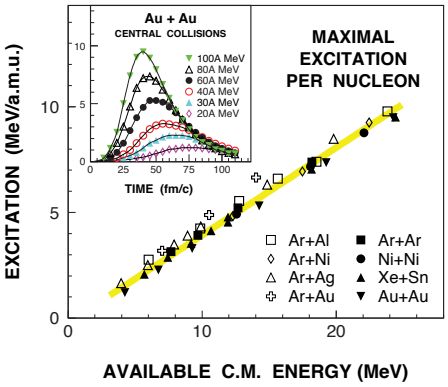

Fig. 1: (Color online.) Simulation results of the thermal excitation energy per nucleon $E_{\rm x}/A$ for central collisions. *Inset*: Time evolution of $E_{\rm x}/A$ for the Au+Au reaction at the indicated energies. At each time step considered are particles that are bound in large fragments, in fact the early compact system.
Main figure: Excitation maxima $(E_{\rm x}/A)_{\rm max}$ as a function of the system available energy $E^{\rm c.m.}_{\rm avail}$ for the mass asymmetric (open symbols) and the mass symmetric (filled symbols) systems studied. The thick grey line is due to the best linear fit to all data points.

diate mass fragments owing to the thermal excitation component $E_{\rm x}$. At energies below $100A$ MeV the compression-decompression process contributes a little in the total (kinetic) energy dissipation in HIR [12]. At the instant at which the maximum $(E_{\rm x}/A)_{\rm max}$ is reached a negligible emission occurs and at energies of our interest it amounts at most 3–5 % of the total system mass [7]. Thus, conjunction of the $(E_{\rm x}/A)_{\rm max}$ with the total (kinetic) energy released in HIR seems to be a natural assumption. One must keep in mind, however, that a simulation maximum is reached prior to although very close (of the order of ∼5–10 fm/c) to the time at which the total momentum distribution becomes locally spherical, i.e., the instant at which the local equilibrium has been reached in each part of the compact subsystem of bound particles [10]. Nevertheless, the system is far from a global equilibrium [7] and comparison with experimental $E_{\rm x}/A$ is not straightforward. Consequently, one must bear in mind that one should limit the comparison to general trend of experimental data, i.e. to the degree of linearity of $(E_{\rm x}/A)$ as a function of $E^{\rm c.m.}_{\rm avail}$ without seeking to reproduce the simulation absolute value. $(E_{\rm x}/A)_{\rm max}$ is reached during the very first reaction phase and if experimental data would display the same slope that could not but be a fortuitous result. Indeed, experimental data is registered at an infinite time. Hence, it reflects an integral of the full reaction history. Anyway, the simulation maxima $(E_{\rm x}/A)_{\rm max}$ should be compared with either the maximal value of $E_{\rm x}/A$ obtained in an experiment or with the most probable value of $E_{\rm x}/A$ depending on the nature of the distribution.

Figure 2 displays a collection of experimental data on $E_{\rm x}/A$ and total energy dissipated in central HIR published in periodics during the last two decades [13–26]. Because energy dependence is crucial for our comparison from the figure are dropped all single-energy results. Each reaction system is depicted by its symbol while the different measurements of the same system are distinguished by color (on line). To avoid of entirely spoiling the figure the error bars, typically of 5–15 %, are not displayed. To guide the eye, points belonging to the same system and the same analysis are connected and they mostly display close-to-linear dependence on $E^{\rm c.m.}_{\rm avail}$. Unlike the simulation result on $(E_{\rm x}/A)_{\rm max}$ (cf. the thick grey line in Fig. 2) the experimental data points span a large domain of the $E_{\rm x}/A$ vs. $E^{\rm c.m.}_{\rm avail}$ plane: The extracted excitations per nucleon lie between one third and almost the full accessible system energy $E^{\rm c.m.}_{\rm avail}$. One may speculate that the different approaches used in extracting from experiments the pertinent information on the global energy deposition in HIR might be at the origin of these much more scattered results. Indeed, in a HIR experiment one does not have a direct access to the excitation energies involved. To obtain $E_{\rm x}/A$ one needs to reconstruct from detected reaction products the total excitation $E_{\rm x}$ of an assumed primary emission source but also the source mass A. There is an evident difficulty to restore the break-up stage using exclusively asymptotic experimental information which is further obscured by an important role played by primary fragments internal excitation causing the in-flight emission. To overcome these uncontrolled issues one has to resort to certain more or less justified physical assumptions or/and to use theoretical predictions as a guide for data analysis. Anyhow, data analyzed on a same

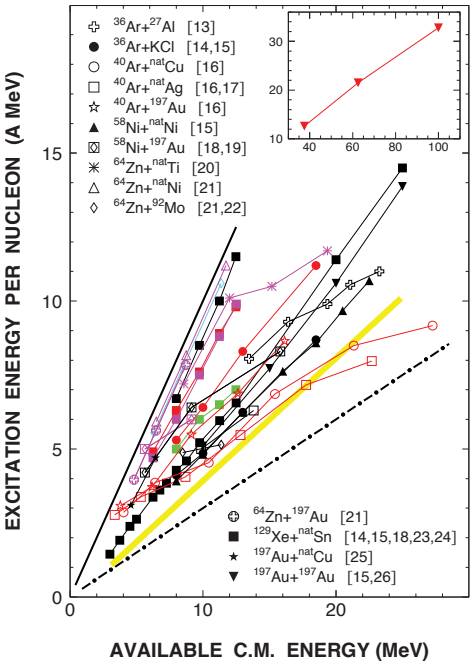

Fig. 2: (Color online.) Experimentally evaluated total excitation energy per nucleon or total dissipated energy per nucleon as a function of system available energy. Each reaction is represented by its own symbol and by color are distinguished different analyses of the same reaction. The thick full line corresponds to the $E_{\rm avail}^{\rm c.m.}$ and displays the upper energy limit which may be reached in HIR while the thick dash-dotted line depicts 30 % of this limit. The only data on the total $E_{\rm x}/A$ above 100A MeV are for the Au+Au reaction at $E_{\rm in}$=150A, 250A and 400A MeV [26]. They are shown in the inset. The axes aspect ratio of both the inset and the main diagram is the same so that the slope in both is the same. The very thick grey line is due to the best linear fit to the simulation results of Fig. 1.

footing seems to fall into much narrower zones of the $E_{\rm avail}^{\rm c.m.}$ vs. $E_{\rm x}/A$ plane.

4 Excitation share in the system available energy

A universal linear dependence of $(E_{\rm x}/A)_{\rm max}$ on $E_{\rm avail}^{\rm c.m.}$ as well as its nearly exact crossing of the origin in Fig. 1 has an important and remarkable consequence: Expressing the value of maximal excitation in percentage of the system available energy one obtains that the relative fraction of $(E_{\rm x}/A)_{\rm max}$ in $E_{\rm avail}^{\rm c.m.}$ has an almost constant value as can be seen in Fig. 3a). The exception to this constancy is for symmetric systems at $E_{\rm in} < E_{\rm F}$ which occurs because when $E_{\rm in}$ decreases below $E_{\rm F}$[1] the value of the maximum $(E_{\rm x}/A)_{\rm max}$ decreases faster than $E_{\rm avail}^{\rm c.m.}$ itself is decreasing. This is a consequence of an ever slower and slower the early compact system energy transformation as $E_{\rm in}$ decreases with an ever more broadened maximum (cf. inset in Fig. 1). Therefore, at these lower $E_{\rm in}$ the maximum $(E_{\rm x}/A)_{\rm max}$ is no more proportional on the same manner to the total energy deposited in HIR as for $E_{\rm in} \gtrsim E_{\rm F}$: These simulation $(E_{\rm x}/A)_{\rm max}$ cannot be compared with an experimental $E_{\rm x}/A$ of fusion reaction, i.e. of adiabatic-like processes. With this restriction in mind, from Fig. 3a) one infers that share of $E_{\rm x}/A$ in $E_{\rm avail}^{\rm c.m.}$ weekly depends on either reaction system or incident energy $E_{\rm in}$ and amounts 0.39±0.03 of $E_{\rm avail}^{\rm c.m.}$. In other words, during the early energy transformation in HIR the maximal excitation energy that may be deposited in the system is a constant which amounts about 40 % of the system available energy. Let us underline that this constancy of the maximum-of-excitation-energy share in available energy is evidenced in the fairly broad range of $E_{\rm in}$ (quotient of the highest and the lowest $E_{\rm avail}^{\rm c.m.}$ covered in the simulation is $\sim$9) and it is nearly independent of system size (studied is the range of $60 \lesssim A_{\rm sys} \lesssim 400$ nucleons) and mass asymmetry ($A_{\rm P} : A_{\rm T}$ is varied between 1:1 and 1:5).

Linear dependence of $E_{\rm x}/A$ on $E_{\rm avail}^{\rm c.m.}$ is not sufficient to obtain a constancy of its fraction in available energy: The line passing through data points should also pass close to the origin of the $E_{\rm avail}^{\rm c.m.}$ vs. $E_{\rm x}/A$ plane. As an example in Fig. 3b) are shown results for the Xe+Sn system which have been

[1] For mass symmetric systems $E_{\rm F}$ corresponds to $E_{\rm avail}^{\rm c.m.} \approx 8A$ MeV.

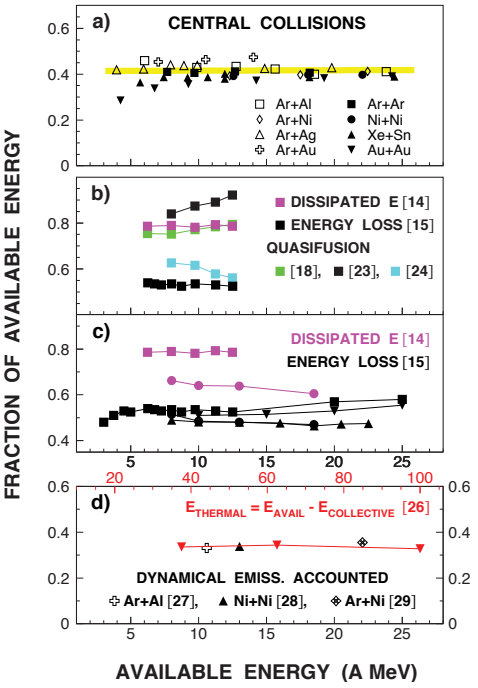

Fig. 3: (Color online.) Ratio of the excitation energy per nucleon and the corresponding $E^{\rm c.m.}_{\rm avail}$ as a function of this same available energy $E^{\rm c.m.}_{\rm avail}$. Symbols used to distinguish different systems are the same as in Fig. 2.
Panel a): Simulation results of Fig. 1.
Panel b): Five different analysis of the Xe+Sn reaction for $25A \leq E_{\rm in} \leq 50A$ MeV.
Panel c): Ratio values reported in the analyses based on the pure kinematical considerations.
Panel d): Ratio values reported in analyses which thoroughly accounted for the pre-equilibrium emission component as well as the results on the total thermal energy reported above $100A$ MeV and for which the abscissae labels above the panel frame are relative to.

extensively studied by the INDRA collaboration. Displayed are five analyses of apparently the same data set for $25A \leq E_{\rm in} \leq 50A$ MeV [14,15,18,23,24]. Each analysis has used its own approach in selecting data by centrality and its own philosophy in extracting the total excitation $E_{\rm x}$ and the primary source mass A. Reported $E_{\rm x}/A$ differ substantially among them: The absolute value at the same $E_{\rm in}$ differs up to 80 %. Moreover, some of presumed single-source (quasifusion) analyses display a rising fraction of $E_{\rm x}/A$ in $E^{\rm c.m.}_{\rm avail}$ as $E_{\rm in}$ increases [18,23], other falling fraction as $E_{\rm in}$ increases [24], whereas the most probable dissipated energy [14] and the total energy loss [15] displays a weak if any dependence on $E_{\rm in}$.

Dissipated energy and total energy loss are the analyses inspired by the kinematical arguments and do not require presumption on the dominant reaction mechanism. Their drawback is in their applicability to the mass-symmetric systems only. Figure 3c) displays results for all systems studied by these two approaches in a fairly broad range of $E_{\rm in}$. The total energy loss within the error bars gives the same constant value for all four systems studied. The results of Figure 3c) are rather weekly depending on $E_{\rm in}$ and may be considered constant. Another example of cases with the constant fraction of $E_{\rm x}/A$ in $E^{\rm c.m.}_{\rm avail}$ is shown in Fig. 3d). Displayed are three single-energy studies that carefully accounted for the copious midrapidity emission [27–29] which occurs during the compact and prior-to-scission reaction phase discussed in Sect. 1 as well as the only $E_{\rm x}/A$ result reported so far above $100A$ MeV. Within blast model extracted is the total thermal energy for the Au+Au reaction from $150A$ to $400A$ MeV [26]. These Au+Au data have recently been revised [30] but a strict linearity of the studied ratio as a function of $E_{\rm in}$ did not change so that the value of our fraction should merely be slightly increased.

5 Conclusions

In conclusion, a semiclassical transport model study of the early reaction phase of central heavy-ion collisions at intermediate energies has been carried out for a variety of system masses, mass asymmetries, and energies below $100A$ MeV. It has been found that the maxima of the excitation energy $E_{\rm x}$ deposited

at this early reaction stage into the reaction system represents a constant fraction of about 40 % of the total center-of-mass available energy of the system $E_{\mathrm{avail}}^{\mathrm{c.m.}}$. In heavy-ion experiments extracted total dissipated energy per nucleon and total energy loss deduced on kinematical arguments display a similar constancy of their share in the system available energy. A similar result may be found in total excitation energy extracted from experimental observations under condition that the pre-equilibrium emission is properly accounted for. This indicates that the stopping power of nuclear matter is significant even below the threshold of nucleon excitation and that it does not change appreciably over a wide range of incident energies, a result corroborated experimentally [31].

References

[1] D. Durand, E. Suraud and B. Tamain, Nuclear Dynamics in the Nucleonic Regime, (Institute of Physics Publishing, Bristol and Philadelphia, 2001).

[2] R. Bass, Nuclear Reactions with Heavy Ions, (Springer, Berlin, 1980).

[3] A. Bonasera, R. Coniglione and P. Sapienza, *Eur. Phys. J.* A **30** (2006) 47.

[4] Ph. Eudes, Z. Basrak and F. Sébille, *Phys. Rev.* C **56** (1997) 2003.

[5] F. Haddad, Ph. Eudes, Z. Basrak and F. Sébille, *Phys. Rev.* C **60** (1999) 031603.

[6] Z. Basrak and Ph. Eudes, *Eur. Phys. J.* A **9** (2000) 207; Ph. Eudes, Z. Basrak and F. Sébille, *Proc. 36th Int. Winter Meeting on Nucl. Phys. (Bormio)* ed. Iori I (University of Milan Press, Milan, 1998), p. 277.

[7] I. Novosel, Z. Basrak, Ph. Eudes, F. Haddad and F. Sébille, *Phys. Lett.* B **625** (2005) 26.

[8] B. Remaud, F. Sébille, C. Grégoire, L. Vinet and Y. Raffray, *Nucl. Phys.* A **447** (1985) 555c; F. Sébille, G. Royer, C. Grégoire, B. Remaud and P. Schuck, *Nucl. Phys.* A **501** (1989) 137.

[9] J. Dechargé and D. Gogny, *Phys. Rev.* C **21** (1980) 1568.

[10] P. Abgrall, F. Haddad, V. de la Mota and F. Sébille, *Phys. Rev.* C **49** (1994) 1040.

[11] V. de la Mota, F. Sébille, M. Farine, B. Remaud and P. Schuck, *Phys. Rev.* C **46** (1992) 677.

[12] J. Pochodzalla, *Prog. Part. Nucl. Phys.* **39** (1997) 443.

[13] J. Péter, *et al. Nucl. Phys.* A **593** (1995) 95.

[14] V. Métivier, *et al.* (INDRA Collaboration), *Nucl. Phys.* A **672** (2000) 357.

[15] G. Lehaut, *Ph.D. Thesis* (Université de Caen, Caen, France, 2009).

[16] Sun Rulin, *et al. Phys. Rev. Lett.* **84** (2000) 43.

[17] E. Vient, *et al. Nucl. Phys.* A **571** (1994) 588.

[18] B. Borderie, *et al.* (INDRA Collaboration), *Nucl. Phys.* A **734** (2004) 495.

[19] N. Bellaize, *et al.* (INDRA Collaboration), *Nucl. Phys.* A **709** (2002) 367.

[20] J.C. Steckmeyer, *et al. Phys. Rev. Lett.* **76** (1996) 4895.

[21] J. Wang, *et al.* (NIMROD Collaboration), *Phys. Rev.* C **72** (2005) 024603.

[22] J. Wang, *et al.* (NIMROD Collaboration), *Phys. Rev.* C **71** (2005) 054608.

[23] N. Le Neindre, *et al.* (INDRA and ALADIN Collaborations), *Nucl. Phys.* A **795** (2007) 47.

[24] E. Bonnet, *et al.* (INDRA and ALADIN Collaborations), *Phys. Rev. Lett.* **105** (2010) 142701.

[25] M. D'Agostino, *et al.* (MULTICS-MINIBALL Collaborations), *Nucl. Phys.* A **724** (2003) 455.

[26] W. Reisdorf, *et al.* (FOPI Collaboration), *Nucl. Phys.* A *612* (1997) 493.

[27] G. Lanzanò, *et al.* (ARGOS Collaboration), *Nucl. Phys.* A *683* (2001) 566.

[28] D. Thériault, *et al.* (INDRA Collaboration), *Phys. Rev.* C *71* (2005) 014610.

[29] D. Doré, *et al.* (INDRA Collaboration), *Phys. Lett.* B *491* (2000) 15.

[30] W. Reisdorf, *et al.* (FOPI Collaboration), *Nucl. Phys.* A *848* (2010) 366.

[31] G. Lehaut, *et al.* (INDRA and ALADIN Collaborations), *Phys. Rev. Lett.* **104** (2010) 232701.